EES Catalysis

MINIREVIEW

View Article Online
View Journal | View Issue

Cite this: *EES Catal.*, 2024, 2, 780

Revisiting group 4–7 transition metals for heterogeneous ammonia synthesis

Wenbo Gao, [ab] Yawei Wang, [ab] Qianru Wang, [ab] Zhaolong Sun, [ab] Jianping Guo *[ab] and Ping Chen [ab]

Received 8th December 2023,
Accepted 31st January 2024

DOI: 10.1039/d3ey00301a

rsc.li/eescatalysis

Ammonia is a key small molecule for manufacturing nitrogen-based fertilizers and organic chemicals and equally important for renewable energy storage and conversion. The available Haber–Bosch ammonia synthesis process using fused iron catalysts operated under harsh conditions is, however, unsustainable. The development of alternative and more efficient approaches to sustainable ammonia production has garnered much attention recently. Most of the prior work has been devoted to the investigation of Fe, Ru or Co-based metal catalysts for ammonia synthesis. In comparison, there are very limited studies on group 4–7 transition metals, because they are prone to form metal nitrides, which are difficult to hydrogenate to ammonia. This mini-review summarizes recent advances in activating these metals for heterogeneous ammonia synthesis. We show that the potential properties of group 4–7 transition metals for ammonia synthesis should be revisited, which may lead to the development of more efficient materials or chemical processes for ammonia production under mild conditions.

Broader context

Ammonia has been not only a key molecule for manufacturing nitrogen-based fertilizers, but also a 'star molecule' for energy storage, conversion and utilization in recent years. Sustainable ammonia production is the most important part of the future ammonia-powered clean energy systems. Although the Haber–Bosch ammonia synthesis process is available and well defined, it can only be operated under very harsh conditions. The development of more energy-efficient approaches and advanced materials for sustainable ammonia synthesis under mild conditions is highly required. The group 4–7 transition metals have the advantage of high affinity to N_2, but the activated N is difficult to convert further to ammonia and thus exhibits low catalytic activities. It is of both scientific significance and practical relevance to make these transition metals active for ammonia synthesis typically under mild conditions. In this mini-review, the recent advances in employing group 4–7 metals (nitrides) for heterogeneous ammonia synthesis are summarized, emphasizing the opportunities in activating these group 4–7 metals for ammonia production.

1. Introduction

There has been recently considerable interest in dinitrogen fixation to ammonia (N_2-to-NH_3), because ammonia is not only an indispensable chemical intermediate for producing nitrogenous fertilizers and organic chemicals, but also a promising carbon-free energy (hydrogen) carrier and fuel.[1–3] Ammonia has the metrics of high hydrogen content (17.8 wt%), high energy density (22.5 MJ kg^{-1} or 15.6 MJ L^{-1}), facile storage and transportation, *etc.* The synthesis, separation, storage, transportation, and utilization of ammonia are important for the forthcoming 'ammonia energy systems'.[4] The artificial ammonia synthesis, the most difficult process, relies highly on the well-defined and centralized Haber–Bosch (H–B) ammonia synthesis process nowadays, which is operated under high-temperature and high-pressure reaction conditions (673–823 K and 10–30 MPa) using an iron-based catalyst. In the 1990s, a carbon supported ruthenium catalyst was used industrially in the KBR advanced ammonia process, known as KAAP. The development of alternative methods and advanced materials for ammonia synthesis typically under mild conditions is a long sought-after goal. This task is further motivated by the requirements of decentralized, distributed, flexible, and high-efficiency ammonia production processes that could be coupled with the isolated and intermittent renewable energy resources.[5]

However, ammonia synthesis under mild conditions is never an easy task. From the viewpoint of thermodynamics, ammonia synthesis from N_2 and H_2 is an exergonic reaction (ΔG° = −32.9 kJ mol^{-1}). The equilibrium ammonia concentration

[a] *Dalian Institute of Chemical Physics, Chinese Academy of Sciences, Dalian, 116023, China. E-mail: guojianping@dicp.ac.cn*
[b] *Center of Materials and Optoelectronics Engineering, University of Chinese Academy of Sciences, Beijing, 100049, China*

reaches 91.5% at 298 K and 1 bar N_2/H_2 pressure. This is, unfortunately, unattainable under normal thermal reaction conditions because of large kinetic barriers. To obtain an exit NH_3 concentration of practical interest (*i.e.*, >10 mol%), high temperatures and pressures are essential even for the commercialized fused iron or Ru catalyst. This contradiction between thermodynamic and kinetic properties of ammonia synthesis reaction lies in at least two aspects.[6] On one hand, the chemical inertness of the N_2 molecule is basically due to the strong N≡N triple bond (942 kJ mol^{-1}), high HOMO–LUMO gap (10.82 eV), and nonpolarity.[7] On the other hand, it is more difficult to maintain a high N hydrogenation rate with a high N_2 dissociation rate, which is restricted by the energy scaling relationship among different adsorbed species and transition states on a specific active site.[8] This relationship gives rise to a classic volcano-type plot for a series of transition metal surfaces between catalytic activity and the adsorption energy of N as illustrated in Fig. 1a. Metals such as Fe and Ru have moderate N adsorption energies and high intrinsic activities and have thus been applied in the ammonia synthesis industry. For elements at the left- or right-hand side of the volcano plot, a lower activity is found because of their either higher or lower N adsorption energy. Specifically, it is hard for the right-hand side metals to activate N_2, although the hydrogenation of N is facile. For the left-hand side metals, it turns out that a high N adsorption energy leads to a low activation energy for N_2 dissociation but a high energy barrier for N hydrogenation to NH_x (x = 1–3) species. As an example, the clean Cr metal surface has a strong N adsorption energy (E_N = −1.8 eV for the Cr(110) surface),[9] and surface science studies showed that the dissociative adsorption of N_2 and formation of surface Cr nitride could take place at 300 K.[10] The formed surface Cr nitride, however, is too stable to be hydrogenated to NH_3 under moderate conditions. These left-hand side metals have high affinity toward N_2, and hence have advantages of N_2 activation and/or dissociation, which has been generally accepted as the rate-determining step in ammonia synthesis reaction. It is thus of both scientific and practical interest to find out whether or how to enhance the catalytic activities of these left-hand side metals.

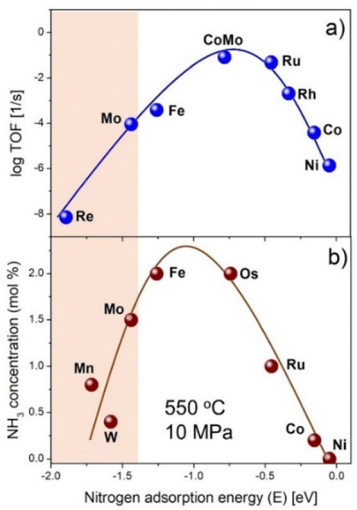

Fig. 1 The classic volcano plot for thermal-catalytic ammonia synthesis. (a) Calculated rate as a function of E_N. (b) The NH_3 concentration data were taken from ref. 28. The N adsorption energies of Mn and W were taken from ref. 9.

Group 4–7 metals such as Ti, V, Cr, Mn, Mo, Nb, *etc.* are located at the left-hand side of the volcano plot and most of them have been rarely used as catalytic materials for thermo-catalytic ammonia synthesis relative to Fe, Ru or Co. However, it is well known that Mo and V are key elements in the cofactors of MoFe and VFe nitrogenases, respectively. The nitrogenase can catalyze N_2 reduction and protonation to NH_3 (NH_4^+) at room temperature and atmospheric pressure although this biological process is also energy-intensive (*ca.* 500 kJ mol^{-1} N_2). There are a large number of soluble transition metal–dinitrogen complexes based on the group 4–7 metals. Among them, a couple of Mo- and V-based complexes have been synthesized and shown to be catalytically active for homogeneous ammonia synthesis.[11] The knowledge on the role of group 4–7 metals in biological or homogenous N_2 fixation would be helpful for the design and development of novel catalysts or functional materials for heterogenous ammonia synthesis. In one early monograph, Aika and Tamaru gave a comprehensive review on the non-iron catalysts including group 4–7 metals for ammonia synthesis before 1995.[12] In this minireview, we would like to summarize the recent advances in the group 4–7 metals for heterogeneous ammonia synthesis, typically heterogeneous thermal catalysis and the chemical looping route. Some strategies to activate the group 4–7 metal nitride surfaces are discussed. We hope this minireview could arouse the interest of the researchers to rethink the role of these transition metals in dinitrogen fixation and ammonia synthesis, which have received far less attention compared with Fe, Ru, and Co metals.

2. Thermo-catalytic ammonia synthesis

Before the invention of the fused iron-based ammonia synthesis catalyst, Mittasch *et al.* had explored various transition metals for ammonia synthesis.[28] They found some of the group 4–7 transition metals such as Mo, W, and Mn are catalytically active for ammonia synthesis at high temperature and pressure (Fig. 1b). With the addition of promoters, the multicomponent iron catalyst was found to be more active than others. Moreover, Fe is much cheaper and easily available, which render it attractive for practical applications. Since then, very little attention has been given to other metals including the group 4–7 metals for ammonia synthesis.

The group 4–7 metals are prone to form thermodynamically stable metal nitrides under the ammonia synthesis reaction conditions. Aika *et al.* studied the mechanism of ammonia synthesis over a molybdenum nitride (Mo_2N) catalyst and proposed that the rate-determining step (RDS) is the chemisorption of N_2, which is retarded by nitrogen atoms on the nitride surface.[29] Boudart *et al.* found the structure sensitivity

Table 1 The ammonia synthesis rates of selected (pre)catalysts containing group 4–7 elements

Samples	NH_3 synthesis rate ($\mu mol\ g^{-1}\ h^{-1}$)	Reaction conditions	WHSV ($ml\ g^{-1}\ h^{-1}$)	Ref.
V	Undetected	673 K, 50 bar	60 000	13
VN	10	673 K, 50 bar	60 000	13
VN	Undetected	573 K, 10 bar	60 000	14
CrN	Undetected	573 K, 10 bar	60 000	14
Mn_4N	Undetected	573 K, 10 bar	60 000	14
Mo_2N	68	673 K, 1 bar	9000	15
Co_3Mo_3N	652	673 K, 1 bar	9000	15
Cs–Co_3Mo_3N	986	673 K, 1 bar	9000	15
Cs–Co_3Mo_3N	5000	673 K, 11 bar	9000	15
Fe–Mo–N	143	673 K, 1 bar	9000	15
Ni_2Mo_3N	383	673 K, 1 bar	12 000	16
Re_3N	430	673 K, 1 bar	9000	17
$CoRe_4$	943	673 K, 1 bar	12 000	18
$ZrCr_2$	580	673 K, 30 bar	60 000	19
$ZrMn_2$	400	673 K, 30 bar	60 000	19
ZrV_2	200	673 K, 30 bar	60 000	19
TaV_2	Undetected	673 K, 30 bar	60 000	19
$Zr(Cr_{0.8}Fe_{0.2})_2$	200	673 K, 30 bar	60 000	19
$Zr(Cr_{0.8}Co_{0.2})_2$	130	673 K, 30 bar	60 000	19
$Zr(Cr_{0.8}Ni_{0.2})_2$	170	673 K, 30 bar	60 000	19
$Zr(Cr_{0.8}Cu_{0.2})_2$	280	673 K, 30 bar	60 000	19
LaMnSi	120	673 K, 1 bar	36 000	20
TiH_2	2800	673 K, 50 bar	60 000	13
$VH_{0.39}$	3200	673 K, 50 bar	60 000	13
$NbH_{0.6}$	400	673 K, 50 bar	60 000	13
ZrH_2	Undetected	673 K, 50 bar	60 000	13
$BaTiO_{2.5}H_{0.5}$	1400	673 K, 50 bar	60 000	21
Ru/$BaTiO_{2.5}H_{0.5}$	28 200	673 K, 50 bar	60 000	22
Fe/$BaTiO_{2.4}H_{0.6}$	14 000	673 K, 50 bar	60 000	22
Co/$BaTiO_{2.5}H_{0.5}$	4000	673 K, 50 bar	60 000	22
LaN–Ru/ZrH_2	5600	623 K, 10 bar	60 000	23
Mn–5LiH	3120	573 K, 10 bar	60 000	14
Mn_4N–LiH	2253	573 K, 10 bar	60 000	14
Mn_4N–NaH	509	573 K, 10 bar	60 000	14
Mn_4N–KH	70	573 K, 10 bar	60 000	14
Mn_4N–CaH_2	224	573 K, 10 bar	60 000	14
Mn_4N–BaH_2	1320	573 K, 10 bar	60 000	14
V–5LiH	273	573 K, 10 bar	60 000	14
Cr–5LiH	3604	573 K, 10 bar	60 000	14
$ZrCr_2$–LiH	750	673 K, 30 bar	60 000	19
CrN–BaH_2	1190	573 K, 10 bar	60 000	24
$K_2[Mn(NH_2)_4]$	1124	573 K, 10 bar	60 000	25
$Rb_2[Mn(NH_2)_4]$	1281	573 K, 10 bar	60 000	25
[BaCrHN]	6860	573 K, 10 bar	60 000	24
Ca_3CrN_3H	3800	673 K, 50 bar	60 000	26
Ru/MgO	310	573 K, 10 bar	60 000	14
Cs–Ru/MgO	1390	573 K, 10 bar	60 000	14
Fe cat.	5400	573 K, 9 bar	36 000	27

and strong ammonia inhibition effects on the Mo_2N catalyst for ammonia synthesis.[30] However, the catalytic activity of Mo-based catalysts is commonly lower than those of Fe-based and Ru-based catalysts. With the advancement of materials science and preparation technology, some active ammonia synthesis catalysts employing the group 4–7 metals have been developed. As shown in Table 1, these catalysts could be divided into three types: alloy or metal nitride catalysts, transition metal hydride-based catalysts, and composite catalysts of alkali (alkaline earth) hydride and transition metals.

2.1 Alloy or metal nitride catalysts

Based on the understanding of the Sabatier principle and concept of scaling relations, it appears that improved ammonia synthesis catalysts with optimum N adsorption energies could be found by alloying group 4–7 metals having high N binding energies with those metals having low N adsorption energies. One typical example is the CoMo catalyst developed by Aika and Jacobsen parallelly in 2000,[31,32] which exhibits a higher activity comparable to those of Fe- and Ru-based catalysts. It should be noted that the CoMo alloy transforms into CoMo nitride (Co_3Mo_3N) under the conditions of ammonia synthesis. Alternatively, it has been suggested that the lattice nitrogen may participate in the catalytic cycle *via* a Mars–van Krevelen-like mechanism.[33,34] This reaction pathway involves the synthesis of ammonia by the hydrogenation of lattice nitrogen leading to nitrogen vacancies, which can be replenished by gaseous N_2. Except for the CoMo nitride catalyst, NiMo and FeMo nitride catalysts were also tested, which are less active than CoMo. The addition of Co can also improve the activity of Re or Re_3N but the formation of a ternary metal nitride phase was not observed.[17]

This approach for catalyst design could also be generalized to other transition metals. For example, rare earth metals can combine with Co, Ru, or Fe forming intermetallic compounds such as $CeCo_3$, $CeRu_2$, and $CeFe_2$ showing high specific activities for ammonia synthesis.[12] Ni metal alone is generally inactive for ammonia synthesis, but recent studies showed that combining Ni with rare earth metals, which transformed into nitrides, can significantly enhance its catalytic activity.[35] Some ternary intermetallic compounds such as LaRuSi, LaCoSi, and LaMnSi have been reported as active catalysts for ammonia synthesis.[20,36,37] The intermetallic compounds containing group 4–7 metals, such as $ZrCr_2$, $ZrMn_2$, and ZrV_2, can absorb both H_2 and N_2, and they have been tested for ammonia synthesis recently and form the intermetallic nitride hydride phase, although their catalytic activities are not high.[19] Wang *et al.* reported that a CoMoFeNiCu high-entropy alloy is active for ammonia decomposition, the reverse reaction of ammonia synthesis.[38] There has been so far little work on high-entropy alloys or high-entropy metal hydrides and nitrides for ammonia synthesis catalysis, which is worthy of future study. The artificial intelligence and machine learning would help guide the design and construction of active alloy, hydride or nitride catalysts. Based on the available data sets of adsorption energies of NH_x species on a number of metal, alloy, or nitride surfaces from the databases such as Open Catalyst, a machine learning model could be trained and used to predict N adsorption energies of other different sites. Combining DFT calculations and machine learning could produce an automated framework that is able to search for active sites approaching the optimum N adsorption energies. If the controlled synthesis of alloy or intermetallic compound materials with specific composition, morphology, and size can be achieved, the N adsorption energy could be finely tuned, which may lead to the development of more active alloy or metal nitride catalysts for ammonia synthesis. However, as discussed before, the catalytic activity will be still limited by the scaling relationships on the transition metal surfaces,[8] and hence it remains unclear whether we could achieve high-efficiency ammonia synthesis under mild conditions by using transition metal-only catalysts.

2.2 Transition metal hydrides

As mentioned above, it is known that early transition metals such as Ti, V, or Cr are inactive for ammonia synthesis at low temperatures and pressures (Table 1) because of their strong metal–N bonds. In organometallic chemistry, the reactivity of transition metals can be manipulated by the selection of different kinds of ligands.[11] A series of transition metal (Ti, V, Cr, Nb *etc.*) hydride complexes have been shown to activate or even cleave N_2 *via* reductive elimination and/or reductive protonation mechanisms.[39] For example, a soluble trititanium hydride cluster cleaves N_2 to form N–H bonds under mild conditions (Fig. 2a).[40] Some heterogeneous metal hydride-based materials for N_2 activation have also been reported. Basset *et al.* reported an isolated silica supported tantalum hydride complex ([(≡Si–O)$_2$Ta–H$_x$, x = 1 or 3]) capable of cleaving N_2 at 523 K forming a Ta amido imido product [(≡SiO)$_2$Ta(═NH)(NH$_2$)] (Fig. 2b).[41] However, the hydrogenation to ammonia was not obtained. A single site Mo hydride supported on silica was shown to be active for ammonia synthesis catalysis at 673 K.[42]

The inclusion of hydrogen into the lattice of transition metals forming metal hydrides has been found to counteract the negative effects of overly strong TM–N bonds and make them more active for ammonia synthesis (Fig. 2c). For example, Kageyama *et al.* found that although $BaTiO_3$ is inactive, the titanium-based hydrides (TiH_2 and $BaTiO_{2.5}H_{0.5}$) could catalyze ammonia synthesis *via* a hydrogen-based Mars–van Krevelen mechanism.[21] After the test, TiH_2 and $BaTiO_{2.5}H_{0.5}$ may change to surface TiN and $BaTiO_{2.5}N_{0.2}H_{0.3}$ oxyhydride–nitride structures, respectively. The presence of hydride in the catalyst phase is demonstrated to be crucial. It has been shown later that vanadium hydride ($VH_{0.39}$) and niobium hydride ($NbH_{0.6}$) are also active for ammonia synthesis, whereas V metal and VN are inactive.[13] However, $VH_{0.39}$ finally turns into a nitride–hydride composition of $VH_{0.44}N_{0.16}$, which should be the active phase. These (oxy)hydrides have also been shown as effective supports for loading Ru, Fe, or Co metals for ammonia synthesis catalysis.[22] The reactions of N_2 with gas-phase transition metal atoms and clusters have been studied and the knowledge may be transferred into the real catalytic systems.[43,44] Ma *et al.* reported that N_2 can be activated by the well-defined $Ta_3N_3H^-$ and $Ta_3N_3^-$ gas-phase clusters yielding $Ta_3N_5H^-$ and $Ta_3N_5^-$, respectively.[45] The presence of hydrogen in $Ta_3N_3H^-$ was suggested to modify the charge distribution and the geometry of $Ta_3N_3H^-$, which is crucial to increase the reactivity. Although these transition metal hydrides or nitride–hydride pre-catalysts exhibit insufficient activities in ammonia synthesis reaction, these results encourage that other group 4–7 metal hydrides or multinary metal hydrides may be worthy of further study as (pre)catalysts for ammonia synthesis.

2.3 Alkali (alkaline earth) hydride-transition metal composite catalysts

It has been proposed that the dissociation of N_2 is retarded by the strong bonded N atoms on transition metal surfaces. Provided the N atoms can be removed by a substance, the reactive sites would be open to N_2 activation, and the substance should be regenerated. The alkali and alkaline earth metal hydrides (denoted hereafter as AH) containing negatively charged hydrogen atoms (H^-) possess this functionality. As an example, lithium hydride (LiH) is able to remove nitrogen atoms from the transition metal nitrides (denoted as TMN) to clean the metal surface. It is also important that LiH can bind N atoms to form $LiNH_2$/Li_2NH species, which can further split H_2 heterolytically to give NH_3 and regenerate LiH.[46] This synergy between TMN and LiH creates a favourable pathway that allows 3d TM–LiH composites to exhibit unexpectedly high catalytic activities typically at lower temperatures. As shown in Fig. 3a, the addition of LiH can increase the activity of neat 3d metals (from V to Ni) by nearly 1–4 orders of magnitude at 573 K and 10 bar pressure.[14] Recent work showed that the addition of LiH can improve the activity of Zr-based intermetallic compounds for ammonia synthesis (Table 1). This promoting effect is more remarkable on the early transition metals V, Cr, and Mn. A more prominent feature is that the catalytic activities of Cr–LiH, Mn–LiH, Fe–LiH, and Co–LiH composite catalysts are quite similar and outperform that of the reference Cs–Ru/MgO catalyst. This activity trend is distinctly different from the volcano plot for the neat transition metals (Fig. 1), suggesting that the presence of LiH weakens the dependence of activity on the identity of transition metals, and the scaling relationships on transition metal surfaces have been

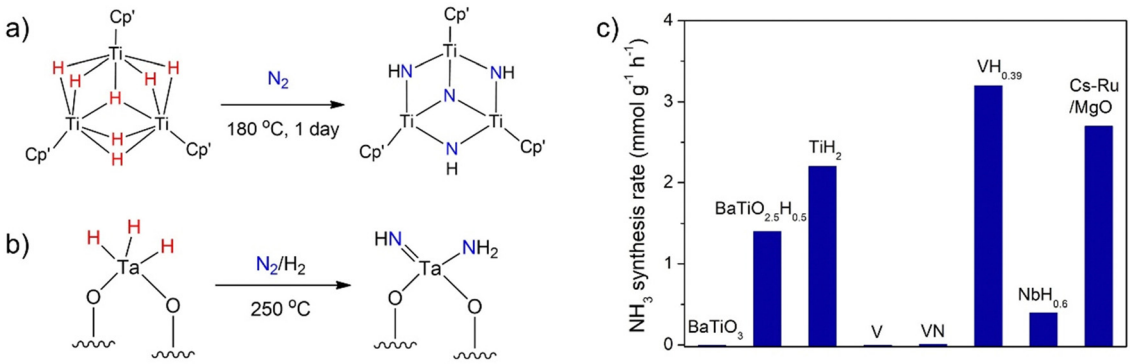

Fig. 2 (a) N_2 cleavage by a soluble trititanium hydride cluster. (b) N_2 activation over an isolated silica supported tantalum hydride complex. (c) NH_3 synthesis rates over a series of early transition metal hydride precatalysts. Reaction conditions: 673 K, 5 MPa.

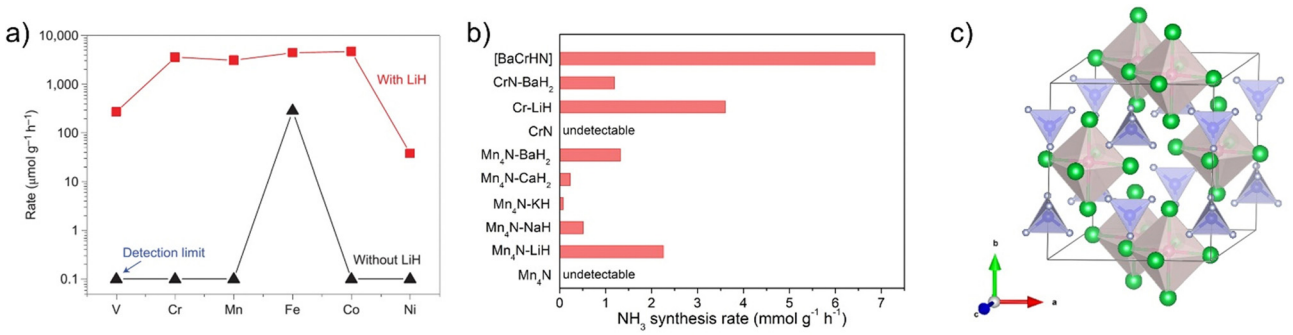

Fig. 3 (a) Impact of LiH on the catalytic activity of 3d transition metals for ammonia synthesis. Reproduced with permission from ref 14. Copyright (2017) Springer Nature. (b) NH_3 production rates of a series of Cr-based and Ru-based catalysts. (c) Crystal structure of Ba_5CrN_4H (Ba, green; H, red; Cr, blue; N, gray).

interfered by the presence of alkali metal hydrides, which are non-transition metal components.

In addition to LiH, other alkali or alkaline earth metal hydrides have also been demonstrated to be able to enhance the catalytic activity of early transition metals. For instance, the ammonia synthesis rate of Mn_4N can be improved significantly by the addition of NaH, KH, CaH_2, or BaH_2 at 573 K and 1 MPa. The Mn_4N–BaH_2 catalyst has an activity of 1320 μmol g_{cat}^{-1} h^{-1}, which is comparable to that of the active Cs–Ru/MgO catalyst. Another important observation is that the activities of Mn_4N–AHs are ranked in the order of Mn_4N–BaH_2 > Mn_4N–LiH > Mn_4N–KH > Mn_4N–CaH_2 > Mn_4N–NaH on the basis of per gram of Mn.[47] Such an order of promoting capability is different from that of the conventional alkali or alkaline earth oxide or hydroxide promoters, *i.e.*, Cs_2O > K_2O > Na_2O > BaO > CaO.[48] Such a difference in promoting order suggests that the function mechanism of alkali and alkaline earth metals depends strongly on their chemical forms. Similarly, CrN has a negligible activity, while the CrN–BaH_2 sample prepared simply by ball-milling CrN and BaH_2 powders can achieve an ammonia synthesis rate of 1190 μmol g_{cat}^{-1} h^{-1}.[24] It is also interesting to see that the phase structures of transition metal nitrides vary with the changes in temperature, pressure, and space velocity, showing a complex dynamic behavior in catalysis.[47] Besides these alkali or alkaline earth metal hydrides, substances with similar functionalities need further study. It would be useful to mention here that the combination of MnN, CrN, VN, *etc.* with alkali or alkaline earth metal amides/imides leads to high catalytic activities for the ammonia decomposition reaction.[49]

Regarding the nature of the active sites of the alkali hydride–transition metal composite catalysts, we found that the alkali or alkaline earth metal hydrides can combine with late transition metals such as Ru or Ir forming complex metal hydrides (Li_4RuH_6, Ba_2RuH_6, K_3RuH_7, Li_3IrH_7 *etc.*).[50,51] Based on this understanding, we supposed that an alkali/alkaline earth-transition metal nitride–hydride species may be formed at the interface of alkali hydrides and transition metal nitrides. To verify this hypothesis, an amorphous barium chromium nitride–hydride catalyst, *i.e.*, [BaCrNH], was synthesized and tested for ammonia synthesis reaction. Experimental results showed that the [BaCrNH] nitride–hydride catalyst exhibits excellent catalytic performance typically under milder conditions (Fig. 3b).[24] The ammonia synthesis rate is *ca.* 4 times that of the reference Cs–Ru/MgO catalyst at 573 K and 1 MPa. The co-existence of Ba and H^- helps to create more reactive N species in the lattice, which is facilely hydrogenated to ammonia and simultaneously leaves a vacant site for N_2 adsorption and activation. The active phase has a Ba_5CrN_4H-like structure containing Ba_6H octahedral and CrN_4 tetrahedral units (Fig. 3c). These reactive H and N species are involved in the ammonia formation process. It has been suggested that N_2 is adsorbed either on the Cr or Ba site of the nitride–hydride catalyst. By heating an orthorhombic nitride Ca_3CrN_3 under hydrogen at 673 K, a hexagonal nitride hydride, Ca_3CrN_3H, was synthesized recently, which exhibited catalytic performance for ammonia synthesis.[26] Because of its well-defined crystal structure, it is beneficial to correlate the surface structure and catalytic performance. It has been suggested that N_2 activation and hydrogenation involves the Ca cations, rather than the Cr sites.[52] Although there is a lack of strong experimental evidence, the catalytic role of transition metals in activating alkali hydrides for N_2 activation is open. Only a handful of nitride–hydride compounds of transition metals have been reported up to now such as $Ca_6Cr_2N_6H$, Ba_3CrN_3H, *etc.*[53,54] There will be much room to develop new nitride–hydride compounds containing various group 4–7 transition metals and alkali or alkaline earth metals for ammonia synthesis as well as other chemical transformations.

3. Chemical looping ammonia synthesis

Chemical looping is a reaction intensification technology by splitting a reaction into two or multiple sub-reactions mediated by certain solid carrier materials. In the chemical looping ammonia synthesis (abbreviated as CLAS) process, N_2 is first fixed by a suitable nitrogen carrier and NH_3 is then harvested by the reactions of N carriers and the hydrogen source. Potential advantages of CLAS include the ability to circumvent the competitive adsorption of N_2 and the H source in the catalytic process and to control process conditions for N_2 fixation and

NH_3 production steps independently.[55] In this sense, CLAS provides an alternative route to circumvent the scaling relations in ammonia synthesis catalysis. Chemical looping ammonia synthesis using early transition metal nitrides as nitrogen carriers could date back to the late 19th century when Tessie du Motay attempted ammonia synthesis *via* a chemical loop based on the interconversion of TiN (or Ti_3N_2) and Ti_5N_3.[56] Haber studied ammonia formation through the stepwise formation and hydrogenation of Mn nitride (Mn_3N_2–Mn), but the ammonia yields were too low for practical applications.[57] Since the advent of the Haber–Bosch catalytic ammonia synthesis process, the development of CLAS has fallen behind. Until the beginning of this century, there was renewed interest in CLAS because it has the potential advantage of utilizing the intermittent renewable energy.[58]

The challenge of CLAS is to find efficient nitrogen carriers and process conditions that produce ammonia at economically acceptable rates. Group 4–7 transition metals enable facile N_2 activation and their nitrides have high and variable nitrogen contents and thus are the main candidate N carrier materials.[55] As shown in Fig. 4, there are basically two types of CLAS processes using transition metal nitrides as nitrogen carriers. The first type uses H_2O as the hydrogen source (Fig. 4a). For example, Pfromm *et al.* designed Cr/CrN/Cr_2O_3 mediated CLAS, which contains three steps: metallic Cr reacts with N_2 to form CrN; CrN hydrolyzes to produce NH_3 and generate Cr_2O_3; and Cr_2O_3 is reduced by CO or H_2 to regenerate metallic Cr.[59] Analogously, Mn/Mn nitride/Mn oxide and Mo/Mo nitride/Mo oxide mediated CLAS processes were also studied.[60,61] Musgrave *et al.* screened more than a thousand metal nitride/metal oxide pairs for CLAS by using high-throughput equilibrium analysis.[62] Many early transition metals had been identified to be promising candidates. The endothermic reduction step generally requires high temperatures (>1000 K) and could use the concentrated solar energy. The second type uses H_2 as the hydrogen source. In this process, NH_3 is produced through the interconversion between N-rich and N-poor nitrides. Michalsky *et al.* studied the $Mn_6N_{2.58}/Mn_4N$ mediated CLAS, but the NH_3 production rate is only 55 μmol g^{-1} h^{-1} at 823 K and 0.1 MPa H_2.[63] Metal doping has been shown to alter the geometrical and electrical structures and chemical properties of N carriers, and thus could boost NH_3 production.[64] Hargreaves *et al.* reported that doping Mn nitride (Mn_3N_2) with low levels of lithium resulted in enhanced reactivity toward hydrogenation at low temperature.[65] With the addition of Co, the conversion rate of lattice N in CrN can be increased by one order of magnitude at 973 K and 0.1 MPa H_2.[66] Gao *et al.* showed that alkali and alkaline earth metal hydrides-imides can be employed as N carriers in a two-step NH_3 loop (eqn (1) and (2)).[55] On this basis, composite N carriers containing both early transition metal nitrides and alkali or alkaline earth metal imides, *e.g.*, Mn_4N–LiH/Mn_2N–Li_2NH and Mn_4N–BaH_2/Mn_2N–BaNH, have been proposed.[67] The Mn nitride not only acts as a nitrogen carrier but also functions as a catalyst enhancing the kinetics of N_2 fixation by alkali hydride to form imide (eqn (1)) and the subsequent hydrogenation of the imide to NH_3 (eqn (2)). The hydrides also facilitate the kinetics of N_2 fixation and subsequent hydrogenation of the Mn nitride. These features make the loop feasible at ambient pressure and temperatures below 300 °C (Fig. 4c). The

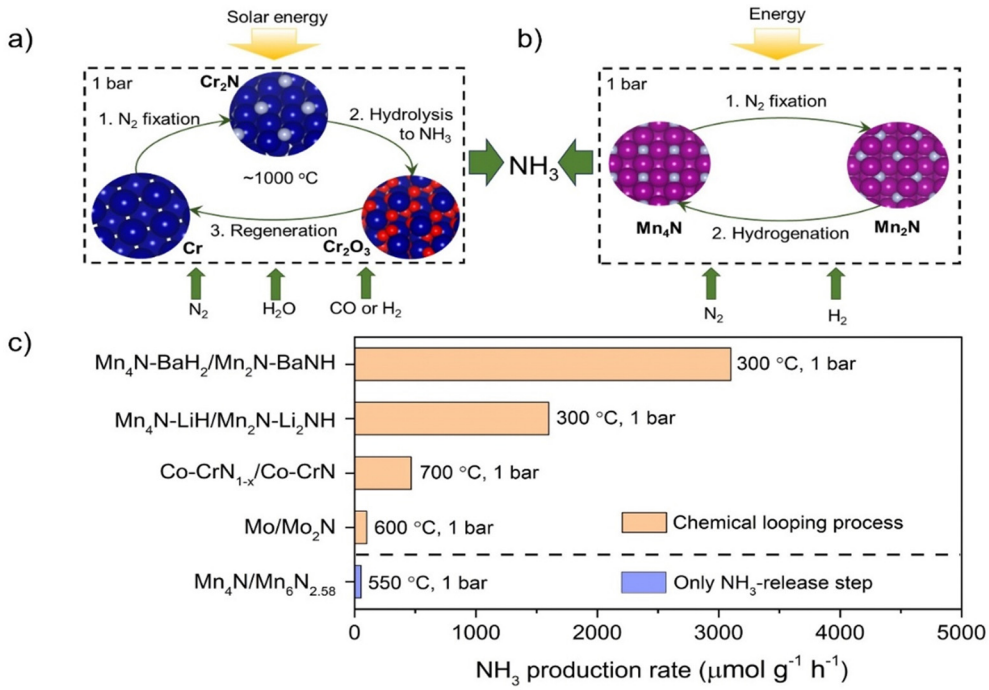

Fig. 4 Two types of chemical looping ammonia synthesis processes using transition metal nitrides as nitrogen carriers. (a) Metal–metal nitride–metal oxide loop (Cr, blue; N, light blue; O, red). (b) N-rich metal nitride–N–lean nitride loop (Mn, purple; N, light blue). (c) Comparison of chemical looping ammonia synthesis rates for selected N carriers.

CLAS performances could be potentially further improved by selecting different couples of transition metal nitrides and alkali or alkaline earth metal imides to optimize the thermodynamic and kinetic properties. On the other hand, the advancement of preparation methods to increase the number of active sites on the surfaces of N carriers could also provide an opportunity to enhance the energy efficiency of CLAS.

$$4LiH + N_2 \rightarrow 2Li_2NH + H_2 \quad (1)$$

$$2Li_2NH + 4H_2 \rightarrow 4LiH + 2NH_3 \quad (2)$$

4. Beyond thermal ammonia synthesis

Besides the thermal activation routes, the interactions of transition metal nitrides with external fields such as electricity, photon, microwave, and plasma would increase freedom to manipulate the properties of metal nitrides toward N_2-to-NH_3.

Electrocatalytic N_2 reduction to NH_3 (eNRR) using group 4–7 transition metals such as ZrN, VN, NbN, CrN, and Mo_2N has been studied both theoretically and experimentally. Theoretical calculation results showed that NH_3 forms on these nitrides by way of a Mars–van Krevelen mechanism.[68–70] The free energy required for the endergonic protonation of surface N to NH_3 can be overcome with an applied bias. On the other hand, since the early transition metals bind N stronger than H, they could be more active toward N_2 reduction than toward the competing hydrogen evolution reaction. However, later studies reported that Mo_2N undergoes fast chemical decomposition in aqueous electrolytes and shows no catalytic activity for the NRR.[71] These controversial results leave open room for the careful study of these transition metal nitrides for the eNRR reaction.

Photo-chemical ammonia synthesis has also received increasing attention recently.[72] Photon-driven nitrogen fixation by titania catalysts was reported decades ago by Schrauzer and Guth, but the efficiency is very low.[73] It has been suggested that oxygen defects and/or Ti^{3+} are the active sites for nitrogen adsorption and activation.[74] Recent studies, however, reported that surface carbon has a strong interaction with N_2, which may assist the N_2 reduction process.[75] Many other oxides, nitrides, and sulfides of group 4–7 metals are semiconductors, which could potentially be used as light-absorbing materials and photocatalysts. For example, Tsang *et al.* reported an Fe-decorated 2D MoS_2 photocatalyst for ammonia synthesis,[76] where the main role of MoS_2 is to generate excited electrons upon light illumination transferring to Fe sites for N_2 activation. Some nitrides such as TiN are plasmonic and they can turn illumination into photothermal heating, which may assist in reactions.[77] Tantalum nitride (Ta_3N_5) has a small band gap (2.1 eV) and is considered to be a promising photocatalyst for solar water splitting under visible light.[78] It is interesting to find out whether Ta_3N_5 and other group 4–7 transition metal nitrides could function both as light absorbing materials and photocatalysts for N_2 reduction to NH_3. On the other hand, the influence of photon illumination on weakening the metal nitrogen bonding is also worthy of future investigation.

5. Outlook

Although the studies of ammonia synthesis have continued for more than one century, the goal of ammonia synthesis under mild conditions has not been achieved. It is not only a scientific task, but also of practical relevance, as ammonia has been considered to be a key energy molecule for the sustainable development of human society. The success of biological N_2 fixation suggests that this goal is not unattainable and would continue to provide valuable inspirations for the future studies on artificial nitrogen conversion processes. We should continue to find ways to tackle the contradictions of thermodynamics and kinetics of ammonia synthesis reaction, which may also have impacts on other chemical reactions. Because of the high affinity of group 4–7 transition metals for nitrogen, they are potential candidate materials. Unfortunately, these metals have not received much attention because there is a lack of powerful strategies to weaken the strong metal–N bond and facilitate the hydrogenation of N species to ammonia. Metal alloying and introduction of non-transition metal elements especially hydrogen (hydride) and alkali (or alkaline earth) metals have been demonstrated to be efficient methods. In addition, the introduction of external fields provides greater flexibility for the development of efficient materials or catalysts to achieve ammonia synthesis under mild conditions.

Artificial intelligence (AI) and machine learning have been believed to be able to accelerate catalyst design by identifying key descriptors correlated with the catalytic performances in recent years.[79–81] For example, an active Cu–Al electrocatalyst for CO_2 reduction to ethylene was predicted using density functional theory calculations in combination with active machine learning.[79] This approach may be used for the studies of catalysts or nitrogen carriers for ammonia production. Applying these approaches is challenging since they rely on large data sets with high accuracy and high reliability, which are often not available typically in the fields of chemical looping, plasma, and electro- and photo-chemical ammonia synthesis processes. Extensive and intensive experimental and theoretical work is still needed at this stage.

Conflicts of interest

There are no conflicts to declare.

Acknowledgements

The authors are grateful for financial support from the National Key R&D Program of China (2021YFB4000400), National Natural Science Foundation of China (Grants No. 21988101, 22279131, 22379139), and Youth Innovation Promotion Association CAS (No. Y2022060 and 2022180).

Notes and references

1 J. G. Chen, R. M. Crooks, L. C. Seefeldt, K. L. Bren, R. M. Bullock, M. Y. Darensbourg, P. L. Holland, B. Hoffman, M. J. Janik, A. K. Jones, M. G. Kanatzidis, P. King,

K. M. Lancaster, S. V. Lymar, P. Pfromm, W. F. Schneider and R. R. Schrock, *Science*, 2018, **360**, eaar6611.
2 J. Guo and P. Chen, *Chem*, 2017, **3**, 709–712.
3 L. Ye, R. Nayak-Luke, R. Bañares-Alcántara and E. Tsang, *Chem*, 2017, **3**, 712–714.
4 F. Chang, W. Gao, J. Guo and P. Chen, *Adv. Mater.*, 2021, **33**, 2005721.
5 W. David, *Ammonia: zero-carbon fertiliser, fuel and energy store*, 2020.
6 J. Guo and P. Chen, *Acc. Chem. Res.*, 2021, **54**, 2434–2444.
7 H.-P. Jia and E. A. Quadrelli, *Chem. Soc. Rev.*, 2014, **43**, 547–564.
8 A. Vojvodic, A. J. Medford, F. Studt, F. Abild-Pedersen, T. S. Khan, T. Bligaard and J. K. Nørskov, *Chem. Phys. Lett.*, 2014, **598**, 108–112.
9 E. Skúlason, T. Bligaard, S. Gudmundsdóttir, F. Studt, J. Rossmeisl, F. Abild-Pedersen, T. Vegge, H. Jónsson and J. K. Nørskov, *Phys. Chem. Chem. Phys.*, 2012, **14**, 1235–1245.
10 P. A. Dowben, A. Miller, H. J. Ruppender and M. Grunze, *Surf. Sci.*, 1988, **193**, 336–352.
11 K. C. MacLeod and P. L. Holland, *Nat. Chem.*, 2013, **5**, 559–565.
12 K.-I. Aika and K. Tamara, in *Ammonia: Catalysis and Manufacture*, ed. A. Nielsen, Springer Berlin Heidelberg, Berlin, Heidelberg, 1995, pp. 103–148, DOI: 10.1007/978-3-642-79197-0_3.
13 Y. Cao, A. Saito, Y. Kobayashi, H. Ubukata, Y. Tang and H. Kageyama, *ChemCatChem*, 2021, **13**, 191–195.
14 P. Wang, F. Chang, W. Gao, J. Guo, G. Wu, T. He and P. Chen, *Nat. Chem.*, 2017, **9**, 64–70.
15 R. Kojima and K.-i Aika, *Appl. Catal., A*, 2001, **218**, 121–128.
16 B. Dragoi, A. Ungureanu, A. Chirieac, C. Ciotonea, C. Rudolf, S. Royer and E. Dumitriu, *Appl. Catal., A*, 2015, **504**, 92–102.
17 R. Kojima and K.-I. Aika, *Appl. Catal., A*, 2001, **209**, 317–325.
18 K. McAulay, J. S. J. Hargreaves, A. R. McFarlane, D. J. Price, N. A. Spencer, N. Bion, F. Can, M. Richard, H. F. Greer and W. Z. Zhou, *Catal. Commun.*, 2015, **68**, 53–57.
19 Y. Cao, Z. Wei, W. Al Maksoud, R. Rai, Y. Kobayashi and H. Kageyama, *Solid State Sci.*, 2023, **145**, 107331.
20 H. Li, Y. Gong, H. Yang, X. Yang, K. Li, J. Wang and H. Hosono, *ChemSusChem*, 2023, **16**, e202301016.
21 Y. Kobayashi, Y. Tang, T. Kageyama, H. Yamashita, N. Masuda, S. Hosokawa and H. Kageyama, *J. Am. Chem. Soc.*, 2017, **139**, 18240–18246.
22 Y. Tang, Y. Kobayashi, N. Masuda, Y. Uchida, H. Okamoto, T. Kageyama, S. Hosokawa, F. Loyer, K. Mitsuhara, K. Yamanaka, Y. Tamenori, C. Tassel, T. Yamamoto, T. Tanaka and H. Kageyama, *Adv. Energy Mater.*, 2018, **8**, 1801772.
23 L. Li, T. Zhang, J. Cai, H. Cai, J. Ni, B. Lin, J. Lin, X. Wang, L. Zheng, C.-T. Au and L. Jiang, *J. Catal.*, 2020, **389**, 218–228.
24 Y. Guan, W. Zhang, Q. Wang, C. Weidenthaler, A. Wu, W. Gao, Q. Pei, H. Yan, J. Cui, H. Wu, S. Feng, R. Wang, H. Cao, X. Ju, L. Liu, T. He, J. Guo and P. Chen, *Chem. Catal.*, 2021, **1**, 1042–1054.
25 H. Cao, J. Guo, F. Chang, C. Pistidda, W. Zhou, X. Zhang, A. Santoru, H. Wu, N. Schell, R. Niewa, P. Chen, T. Klassen and M. Dornheim, *Chem. – Eur. J.*, 2017, **23**, 9766–9771.
26 Y. Cao, M. A. Kirsanova, M. Ochi, W. Al Maksoud, T. Zhu, R. Rai, S. Gao, T. Tsumori, S. Kobayashi, S. Kawaguchi, E. Abou-Hamad, K. Kuroki, C. Tassel, A. M. Abakumov, Y. Kobayashi and H. Kageyama, *Angew. Chem., Int. Ed.*, 2022, **61**, e202209187.
27 M. Kitano, Y. Inoue, M. Sasase, K. Kishida, Y. Kobayashi, K. Nishiyama, T. Tada, S. Kawamura, T. Yokoyama, M. Hara and H. Hosono, *Angew. Chem., Int. Ed.*, 2018, **57**, 2648–2652.
28 A. Mittasch and W. Frankenburg, in *Adv. Catal.*, ed. W. G. Frankenburg, V. I. Komarewsky and E. K. Rideal, Academic Press, 1950, vol. 2, pp. 81–104.
29 K.-i Aika and A. Ozaki, *J. Catal.*, 1969, **14**, 311–321.
30 L. Volpe and M. Boudart, *J. Phys. Chem.*, 1986, **90**, 4874–4877.
31 C. J. H. Jacobsen, *Chem. Commun.*, 2000, 1057–1058, DOI: 10.1039/b002930k.
32 K. Ryoichi and A. Ken-ichi, *Chem. Lett.*, 2000, 514–515.
33 D. McKay, D. H. Gregory, J. S. J. Hargreaves, S. M. Hunter and X. Sun, *Chem. Commun.*, 2007, 3051–3053.
34 S. M. Hunter, D. H. Gregory, J. S. Hargreaves, M. Richard, D. Duprez and N. Bion, *ACS Catal.*, 2013, **3**, 1719–1725.
35 T.-N. Ye, S.-W. Park, Y. Lu, J. Li, M. Sasase, M. Kitano, T. Tada and H. Hosono, *Nature*, 2020, **583**, 391–395.
36 J. Z. Wu, J. Li, Y. T. Gong, M. Kitano, T. Inoshita and H. Hosono, *Angew. Chem., Int. Ed.*, 2019, **58**, 825–829.
37 Y. T. Gong, H. C. Li, J. Z. Wu, X. Y. Song, X. Q. Yang, X. B. Bao, X. Han, M. Kitano, J. J. Wang and H. Hosono, *J. Am. Chem. Soc.*, 2022, **144**, 8683–8692.
38 P. F. Xie, Y. G. Yao, Z. N. Huang, Z. Y. Liu, J. L. Zhang, T. Y. Li, G. F. Wang, R. Shahbazian-Yassar, L. B. Hu and C. Wang, *Nat. Commun.*, 2019, **10**, 12.
39 Q. Wang, Y. Guan, J. Guo and P. Chen, *Cell Rep. Phys. Sci.*, 2022, **3**, 100779.
40 T. Shima, S. Hu, G. Luo, X. Kang, Y. Luo and Z. Hou, *Science*, 2013, **340**, 1549–1552.
41 P. Avenier, M. Taoufik, A. Lesage, X. Solans-Monfort, A. Baudouin, A. de Mallmann, L. Veyre, J.-M. Basset, O. Eisenstein, L. Emsley and E. A. Quadrelli, *Science*, 2007, **317**, 1056–1060.
42 L. M. Azofra, N. Morlanés, A. Poater, M. K. Samantaray, B. Vidjayacoumar, K. Albahily, L. Cavallo and J.-M. Basset, *Angew. Chem., Int. Ed.*, 2018, **57**, 15812–15816.
43 Z. Luo, A. W. Castleman, Jr. and S. N. Khanna, *Chem. Rev.*, 2016, **116**, 14456–14492.
44 P. Wang, H. Xie, J. Guo, Z. Zhao, X. Kong, W. Gao, F. Chang, T. He, G. Wu, M. Chen, L. Jiang and P. Chen, *Angew. Chem., Int. Ed.*, 2017, **56**, 8716–8720.
45 Y. Zhao, J. T. Cui, M. Wang, D. Y. Valdivielso, A. Fielicke, L. R. Hu, X. Cheng, Q. Y. Liu, Z. Y. Li, S. G. He and J. B. Ma, *J. Am. Chem. Soc.*, 2019, **141**, 12592–12600.
46 D. H. Gregory, *J. Mater. Chem.*, 2008, **18**, 2321–2330.
47 F. Chang, Y. Guan, X. Chang, J. Guo, P. Wang, W. Gao, G. Wu, J. Zheng, X. Li and P. Chen, *J. Am. Chem. Soc.*, 2018, **140**, 14799–14806.
48 K.-i Aika, T. Takano and S. Murata, *J. Catal.*, 1992, **136**, 126–140.

49 J. Guo, P. Wang, G. Wu, A. Wu, D. Hu, Z. Xiong, J. Wang, P. Yu, F. Chang, Z. Chen and P. Chen, *Angew. Chem., Int. Ed.*, 2015, **54**, 2950–2954.
50 Q. Wang, H. Wen, Y. Guan, S. Zhang, W. Gao, J. Guo and P. Chen, *ACS Catal.*, 2023, **13**, 9882–9890.
51 H. Yan, W. Gao, Q. Wang, J. Guo and P. Chen, *Faraday Discuss.*, 2023, **243**, 55–64.
52 Y. Cao, E. Toshcheva, W. Almaksoud, R. Ahmad, T. Tsumori, R. Rai, Y. Tang, L. Cavallo, H. Kageyama and Y. Kobayashi, *ChemSusChem*, 2023, **16**, e202300234.
53 M. S. Bailey, M. N. Obrovac, E. Baillet, T. K. Reynolds, D. B. Zax and F. J. DiSalvo, *Inorg. Chem.*, 2003, **42**, 5572–5578.
54 N. W. Falb, J. N. Neu, T. Besara, J. B. Whalen, D. J. Singh and T. Siegrist, *Inorg. Chem.*, 2019, **58**, 3302–3307.
55 W. B. Gao, J. P. Guo, P. K. Wang, Q. R. Wang, F. Chang, Q. J. Pei, W. J. Zhang, L. Liu and P. Chen, *Nat. Energy*, 2018, **3**, 1067–1075.
56 J. R. Jennings, *Catalytic ammonia synthesis: fundamentals and practice*, Springer Science & Business Media, 1991.
57 F. Haber and G. Van Oordt, *Z. Anorg. Allg. Chem.*, 1905, **44**, 341–378.
58 M. E. Gálvez, M. Halmann and A. Steinfeld, *Ind. Eng. Chem. Res.*, 2007, **46**, 2042–2046.
59 R. Michalsky and P. H. Pfromm, *Sol. Energy*, 2011, **85**, 2642–2654.
60 R. Michalsky, P. H. Pfromm and A. Steinfeld, *Interface Focus*, 2015, **5**, 20140084.
61 R. Michalsky, B. J. Parman, V. Amanor-Boadu and P. H. Pfromm, *Energy*, 2012, **42**, 251–260.
62 C. J. Bartel, J. R. Rumptz, A. W. Weimer, A. M. Holder and C. B. Musgrave, *ACS Appl. Mater. Interfaces*, 2019, **11**, 24850–24858.
63 R. Michalsky, A. M. Avram, B. A. Peterson, P. H. Pfromm and A. A. Peterson, *Chem. Sci.*, 2015, **6**, 3965–3974.
64 N. Shan, C. Huang, R. T. Lee, N. Manavi, L. Xu, V. Chikan, P. H. Pfromm and B. Liu, *ChemCatChem*, 2020, **12**, 2233–2244.
65 S. Laassiri, C. D. Zeinalipour-Yazdi, C. R. A. Catlow and J. S. J. Hargreaves, *Appl. Catal., B*, 2018, **223**, 60–66.
66 S. Wang, F. Gong, Q. Zhou, Y. Xie, H. Li, M. Li, E. Fu, P. Yang, Y. Jing and R. Xiao, *Appl. Catal., B*, 2023, **339**, 123134.
67 S. Feng, W. Gao, Q. Wang, Y. Guan, H. Yan, H. Wu, H. Cao, J. Guo and P. Chen, *J. Mater. Chem. A*, 2021, **9**, 1039–1047.
68 Y. Abghoui and E. Skúlason, *J. Phys. Chem. C*, 2017, **121**, 6141–6151.
69 X. Ren, G. Cui, L. Chen, F. Xie, Q. Wei, Z. Tian and X. Sun, *Chem. Commun.*, 2018, **54**, 8474–8477.
70 X. Yang, J. Nash, J. Anibal, M. Dunwell, S. Kattel, E. Stavitski, K. Attenkofer, J. G. Chen, Y. Yan and B. Xu, *J. Am. Chem. Soc.*, 2018, **140**, 13387–13391.
71 B. Hu, M. Hu, L. Seefeldt and T. L. Liu, *ACS Energy Lett.*, 2019, **4**, 1053–1054.
72 A. J. Medford and M. C. Hatzell, *ACS Catal.*, 2017, **7**, 2624–2643.
73 G. N. Schrauzer and T. Guth, *J. Am. Chem. Soc.*, 1977, **99**, 7189–7193.
74 H. Hirakawa, M. Hashimoto, Y. Shiraishi and T. Hirai, *J. Am. Chem. Soc.*, 2017, **139**, 10929–10936.
75 B. M. Comer, Y.-H. Liu, M. B. Dixit, K. B. Hatzell, Y. Ye, E. J. Crumlin, M. C. Hatzell and A. J. Medford, *J. Am. Chem. Soc.*, 2018, **140**, 15157–15160.
76 J. Zheng, L. Lu, K. Lebedev, S. Wu, P. Zhao, I. J. McPherson, T. S. Wu, R. Kato, Y. Li, P.-L. Ho, G. Li, L. Bai, J. Sun, D. Prabhakaran, R. A. Taylor, Y. L. Soo, K. Suenaga and S. C. E. Tsang, *Chem Catal.*, 2021, **1**, 162–182.
77 D. F. Swearer, N. R. Knowles, H. O. Everitt and N. J. Halas, *ACS Energy Lett.*, 2019, **4**, 1505–1512.
78 J. Eichhorn, S. P. Lechner, C. M. Jiang, G. Folchi Heunecke, F. Munnik and I. D. Sharp, *J. Mater. Chem. A*, 2021, **9**, 20653–20663.
79 M. Zhong, K. Tran, Y. Min, C. Wang, Z. Wang, C.-T. Dinh, P. De Luna, Z. Yu, A. S. Rasouli, P. Brodersen, S. Sun, O. Voznyy, C.-S. Tan, M. Askerka, F. Che, M. Liu, A. Seifitokaldani, Y. Pang, S.-C. Lo, A. Ip, Z. Ulissi and E. H. Sargent, *Nature*, 2020, **581**, 178–183.
80 Y. Guo, X. He, Y. Su, Y. Dai, M. Xie, S. Yang, J. Chen, K. Wang, D. Zhou and C. Wang, *J. Am. Chem. Soc.*, 2021, **143**, 5755–5762.
81 F. Göltl, *J. Phys. Chem. C*, 2022, **126**, 3305–3313.